Arabian Journal of Geosciences (2019) 12:34
https://doi.org/10.1007/s12517-018-4158-2

ORIGINAL PAPER

Campanian–Maastrichtian unconformities and rudist diagenesis, Aruma Formation, central Saudi Arabia

Sacit Özer[1] · Abdelbaset S. El-Sorogy[2,3] · Mohammad E. Al-Dabbagh[2] · Khaled Al-Kahtany[2]

Received: 11 October 2017 / Accepted: 14 December 2018

Abstract
The Upper Cretaceous Aruma Formation is widely distributed in central Saudi Arabia and consists of three members, from base to top, the Khanasir Limestone Member, the Hajajah Limestone Member, and the Lina Shale Member. It disconfomably overlies the Cenomanian Wasia Formation (middle Turonian, the "Wasia-Aruma break"). Two unconformities were recorded within and at the top of the Aruma Formation: (a) "the lower Campanian unconformity" between the Khanasir Limestone Member and the Hajajah Limestone Member and (b) "the pre-Cenozoic unconformity" between the Lina Shale Member and the Paleogene Umm er Radhuma Formation. The comparison between these unconformities and those recorded on the Arabian Plate was emphasized. A lenticular rudist biostrome in the uppermost part of the Khanasir Limestone Member consists mainly of the radiolitids and sparse canaliculated rudists in life position. However, rudists are entirely fragmented in the lower limestone and are very rare in the upper limestone of the Hajajah Limestone Member. Loose right valves of radiolitids from the Campanian Khanasir Member have underwent diagenetic alterations, such as fragmentation and compaction, micritization, bioerosion, and micritic calcite cement, which indicates marine diagenetic stage, while very limited silicification, dolomitization, and dissolution suggest the meteoric diagenetic environments with arid climates. Isopachus and equant calcite cement and neomorphism may be showed the fresh pharetic zone related with subaerial unconformities.

Keywords Aruma Formation · Upper Cretaceous · Unconformities · Diagenesis · Rudist bivalves · Saudi Arabia

Introduction

In Saudi Arabia, rudists were first described from the Campanian Khanasir Limestone Member of the Aruma Formation by El-Asa'ad (1983a, b, 1987, 1991) and Skelton and El-Asa'ad (1992). In his study on rudist faunas from the Upper Cretaceous of central Saudi Arabia, El-Asa'ad (1987) interpreted an inner sublittoral, warm marine paleoenvironment for the Upper Cretaceous rudist biostromal limestone. This paleoenvironment was characterized by firm, stable substrate surfaces subjected to periodically intense wave and current action, within the photic zone, abundant food supply but with minimal terrigenous input. More recently, Al-Kahtany et al. (2016) presented the stratigraphy and depositional environments of the Aruma Formation. Despite these paleontologic, stratigraphic, and facies data on the rudist-bearing Aruma Formation, no information exists on the diagenetic features of the Campanian rudists, which are abundantly exposed in the Aruma Formation.

Upper Cretaceous rudists were widely distributed throughout the northern and southern margins of the Mediterranean Tethys (Philip 1982, 1985; Steuber and Löser 2000; Steuber 2002). They are described from the Cenomanian–Turonian sequences of Algeria, Tunisia, Egypt, Jordan, and Lebanon and the Campanian–Maastrichtian of Tunisia, Somalia, Oman, UAE, Saudi Arabia, SE Turkey, Iraq, and Iran on the African–Arabian plate (or platform) (see Steuber 2002; Chikhi-Aouimeur 2010; Steuber et al. 2009; Khazei et al. Khazaei et al. 2010; Saber et al. 2009; Özer 2010; Bandel and Salameh 2013; Özer et al. 2013; Özer and Fayez 2015; Özer and Ahmad 2016). Rudists are important datums for

✉ Sacit Özer
sacit.ozer@deu.edu.tr

[1] Geological Engineering Department, Engineering Faculty, Dokuz Eylul University, 35160 Buca Campus, İzmir, Turkey

[2] Geology and Geophysics Department, College of Science, King Saud University, Riyadh, Saudi Arabia

[3] Geology Department, Faculty of Science, Zagazig University, Zagazig, Egypt

Published online: 08 January 2019

establishing relative sea level and the diagenetic processes of the rudist-bearing limestones, rudist reefs, and especially the economic potential of the Upper Cretaceous successions in the African–Arabian plate. Studies of the diagenesis of rudists of this region were mainly based on specimens embedded in limestones (Negra 1984; M'Rabet et al. 1986; Braun and Hirsch 1994; Alsharhan 1995; Aqrawi et al. 1998; Touir and Soussi 2003; Mansour 2004; Sadooni 2005; Negra et al. 2009; Hajıkazemi et al. 2010; Al-Mohammad 2012; Ghanem and Kuss 2013; Shakeri 2013; Asghari and Adabi 2014; Benyoucef et al. 2016). Loose specimens of Cenomanian caprinids and radiolitids are described from northeastern Jordan by Özer and Ahmad (2016). However, the complete diagenetic alterations of these loose rudist specimens have yet to be studied. Rudist material from the Campanian of the Khanasir Limestone Member of the Aruma Formation in central Saudi Arabia allows us to present the diagenetic processes affecting the loose rudist specimens. Because of the wide geographic distribution of rudist associations and the economic reservoir potential of Upper Cretaceous rudist-bearing limestones on the Arabian platform, the diagenetic data obtained from this study may be relevant on a wider geographic scale and to a wider audience of sedimentary petrographers.

This study focuses on diagenetic alterations of loose radiolitid rudists of the Campanian Khanasir Limestone Member and their relationship to sea-level changes and unconformities in the Aruma Formation, central Saudi Arabia (Fig. 1). Interpretations and discussion of the diagenetic environments according to the diagenetic features are also emphasized.

Material and methods

The rudist specimens were collected from a rudist biostrome that caps the Khanasir Limestone Member at the following two localities in the northeast of Riyadh (Figs. 1, 2, 3):

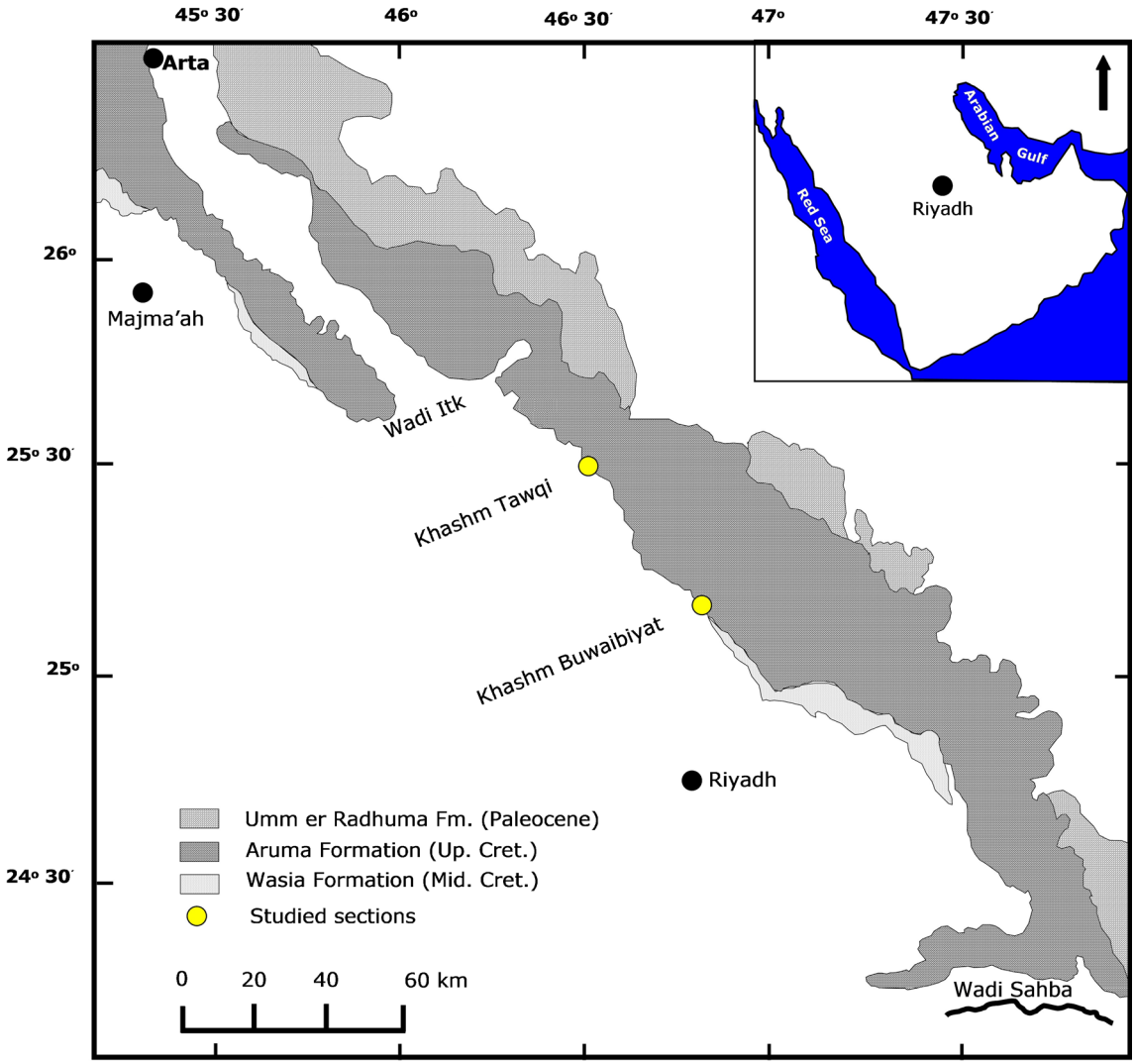

Fig. 1 Geological map of Upper Cretaceous and Paleogene units showing the studied localities (simplified after Gameil and El-Sorogy 2015)

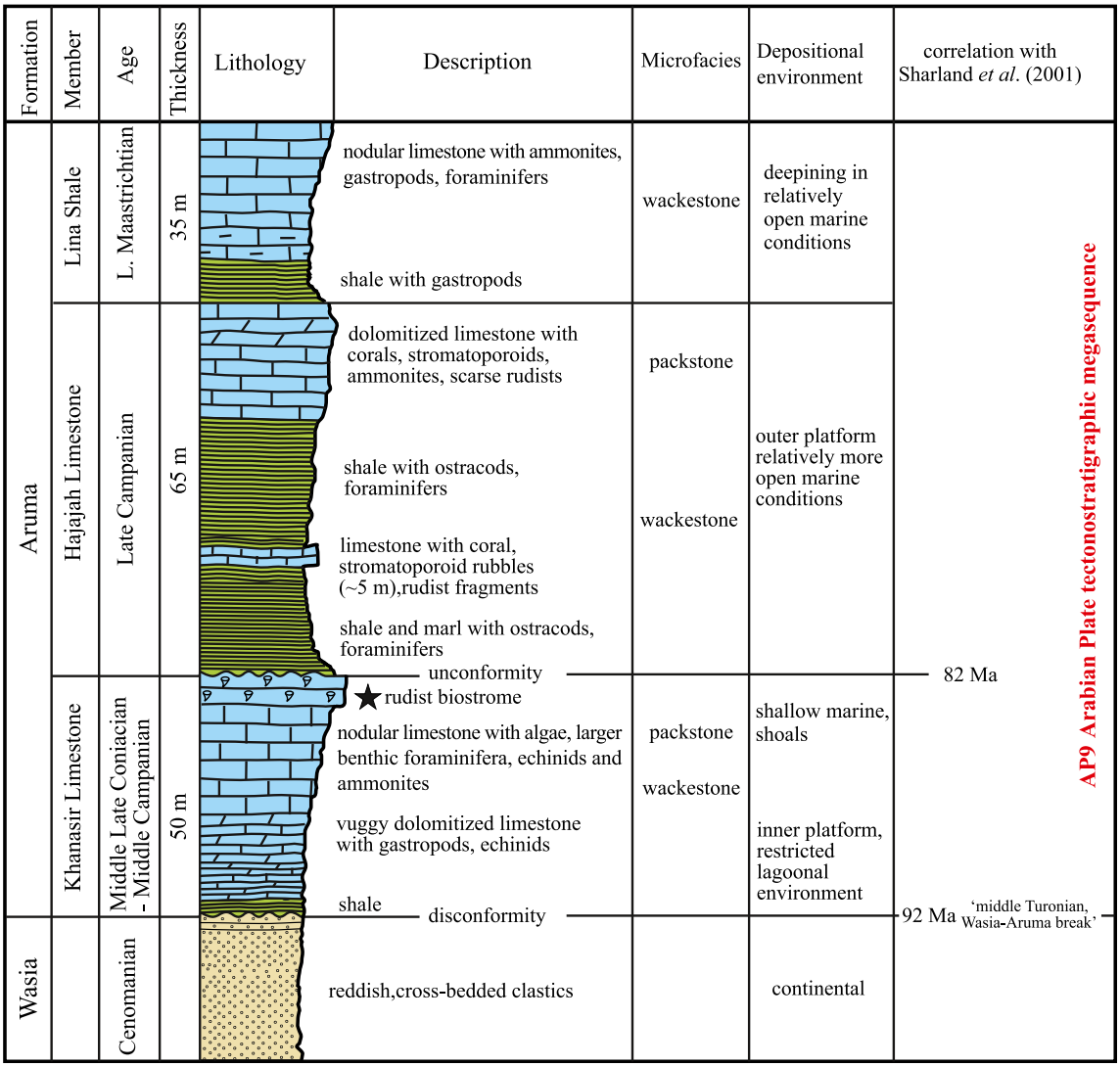

Fig. 2 Generalized stratigraphic section showing the lithologic, microfacies, and depositional environment of the Aruma Formation (Al-Kahtany et al. 2016). Black asterisk shows the location of the collected Radiolitid specimens in the rudist biostrome of the Khanasir Limestone Member of the Aruma Formation

1) Khashm Buwaibiyat on dip-slope surfaces near the crest of the escarpment on either side of the road that trends north–northeast to Rumhiyah at the intersection of latitude 25° 12′ 12″ N and longitude 46° 49′ 27″ E.
2) Khashm Tawqi to the northwest of Khashm Buwaibiyat at the intersection of latitude 25° 27′ 11″ N and longitude 46° 30′ 08″ E, where the same biostromal horizon crops out on the slopes and in gullies beside the road that cuts through the escarpment.

Thirty-seven representative transversal, radial, and tangential thin sections were prepared from right valve specimens (40 *Durania*, 12 *Bournonia*, and 8 *Biradiolites*). Loose specimens were studied to better understand the diagenetic features of the calcitic outer shell layer, the original aragonitic internal shell layer and the body cavity-fill in laboratories at the King Fahd University of Petroleum and Minerals and at the Dokuz Eylul University, Geological Engineering Department, respectively. Valves were tested with HCL to determine the change of carbonate in the outer shell layer and also the presence or absence of carbonate in the sediment filling the body cavity.

Taxonomic descriptions of the radiolitids are not the subject of this study because they seem to be similar to those of the Caribbean Province, but they need a careful study for presentation, so that the studied specimens are identified only at the genus level.

XRD analyses were conducted in the laboratory of the Dokuz Eylul University, İzmir, to determine the mineralogical composition of two samples of the yellowish deposits filling the body cavity of the *Durania* and *Biradiolites* specimens.

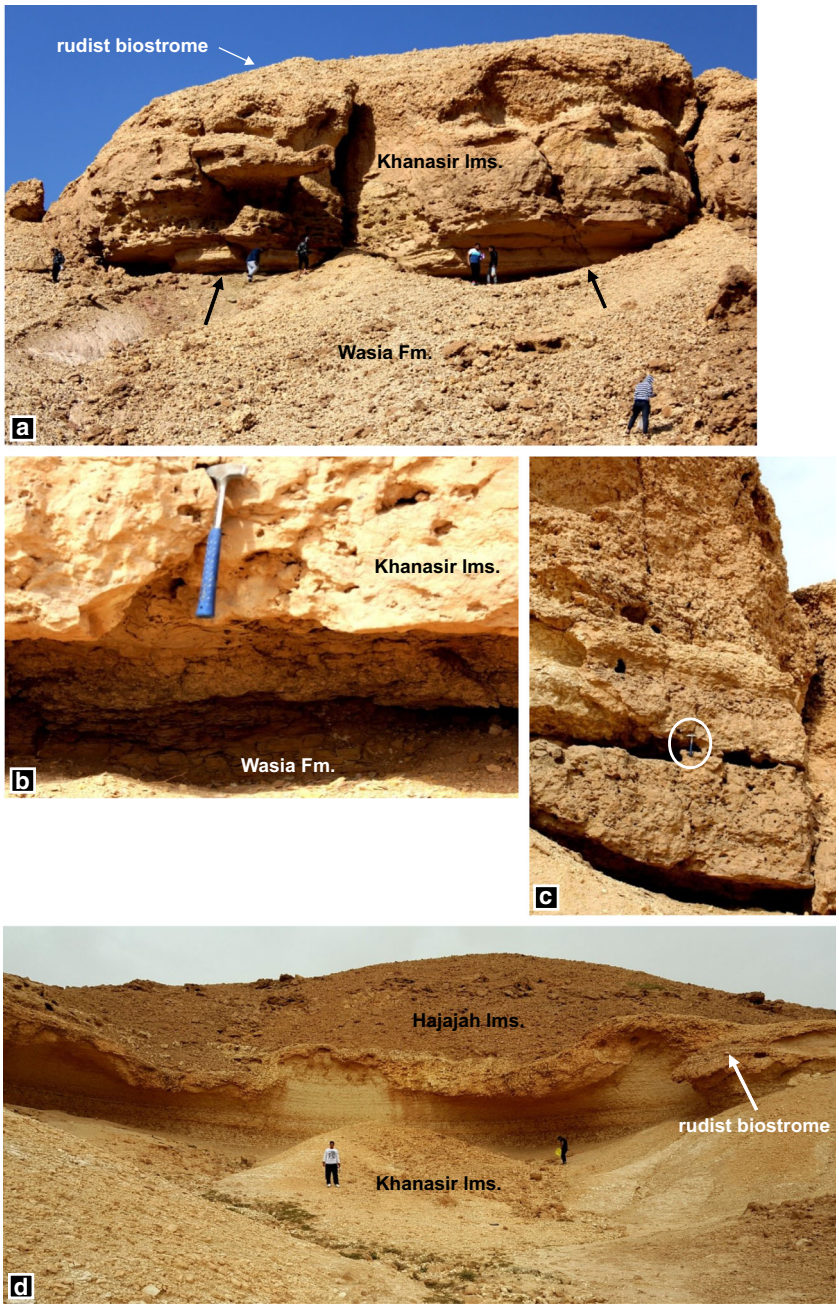

Fig. 3 Outcrop photographs showing the relationships of the Wasia Formation, the Khanasir Limestone Member, and the Hajajah Limestone Member of the Aruma Formation and the rudist biostrome at Khashm Al Buwaybiyat: **a** The black arrows indicate the contact between the Wasia Formation and the Khanasir Limestone Member; the rudist biostrome is at the top of the Khanasir Limestone Member. **b** Close-up of the contact between the Wasia Formation and the Khanasir Limestone Member. **c** Close view of the rudist biostrome consisting mainly of radiolitids in life position; note very low dip; hammer indicates scale. **d** Note the undulating erosional surface between the Khanasir Limestone Member and the Hajajah Limestone Member, and the rudist biostrome is at the top of the Khanasir Limestone Member showing the lateral thickness change

Rudist specimens are photographed and stored in the Museum of the Geology and Geophysics Department, College of Science, King Saud University, Saudi Arabia, and the Geological Engineering Department of the Dokuz Eylül University, İzmir, Turkey.

Geological setting and stratigraphy

The Aruma Formation was named by Steineke and Bramkamp (1952) for Upper Cretaceous rocks cropping out on the Al'Aramah Plateau, a broad upland surface related to the easternmost Najd escarpments in central Saudi Arabia. The formation is widely distributed in Saudi Arabia (Fig. 1) along the western edge of the Rub' Al-Khali east of Riyadh and northward extending to the southern Iraqi border (Powers et al. 1966; Powers 1968; El-Asa'ad 1977, 1983a, b; Harris et al, 1984; Alsharhan and Nairn 1990; Skelton and El-Asa'ad 1992; El-Nakhal and El-Naggar 1994; Sharland et al. 2001; Ziegler 2001; Philip et al. 2002; GameiL and El-Sorogy 2015; Al-Kahtany et al. 2016). The Aruma Formation was subdivided by El-Asa'ad (1977, 1983a, b) into three members: the Khanasir Limestone Member, overlain by the Hajajah Limestone Member which is overlain by the Lina Shale Member (Fig. 2). This subdivision of the formation was used by

Skelton and El-Asa'ad (1992), El-Nakhal and El-Naggar (1994), Sharland et al. (2001), Philip et al. (2002), Gameil and El-Sorogy (2015), and Al-Kahtany et al. (2016). The base of the Aruma Formation is the unconformable contact with the underlying Cenomanian Wasia Formation (Figs. 2, 3a). The uppermost part of the Wasia Formation consists of red and green siltyshale overlying reddish, fine- to medium-grained, cross-bedded sandstone providing the evidence of emergence. The contact is readily placed between the reddish sandstone below and coarsely crystalline dolomite and dolomitic limestone above (Fig. 3b). This "middle Turonian unconformity" was called the "Wasia-Aruma break," and it was suggested to be the result of localized uplift following ophiolitic obduction on the northeastern margin of the Arabian plate, around Kuwait, Iraq, Syria, Jordan, Lebanon, SE Turkey, UAE, and Oman (Sharland et al. 2001). The upper limit of the Aruma Formation is the disconformity between yellow-brown dolomitic shale below and gray crystalline *Lockhartia*-bearing dolomite of the Middle Paleocene–Lower Eocene Umm er Radhuma Formation above. This break is well-known in the Arabian Plate as the "pre-Cenozoic Unconformity," around Kuwait, Iraq, Syria, Qatar, UAE, and Oman (Sharland et al. 2001).

From the base to the top, the Khanasir Limestone Member consists of the following: (1) shale and reddish-brown, dark red to brown, vuggy dolomitized limestone (15–20 m) with a few small pebbles and abundant vugs, many filled with white coarsely crystalline calcite, badly preserved gastropods and echinoids; (2) cream-colored, chalky, slightly dolomitized nodular limestone (20–25 m) with dacycladacean algae, larger benthic foraminifera, echinoids, and ammonites; and (3) a rudist biostrome (2–4.5 m) (Figs. 3a–d, 4a). El-Asa'ad (1983b) recognized the following four faunal zones in the Khanasir Limestone Member: the *Tissotia* Assemblage Zone (Coniacian), the *Lopha/Ostrea* Assemblage Zone (Santonian), the *Sphaerulites/Biradiolites* Assemblage Zone = *Durania* Assemblage Zone (Santonian), and the *Cardium/Protocardia* Assemblage Zone = the *Monolepidorbis sanctae-pelagiae/Orbitoides tissoti* Local Range Zone (Campanian). Also, El-Asa'ad (1983b) identified two larger foraminifers, *Monolepidorbis sanctae-pelagiae* Astre and *Orbitoides tissoti*

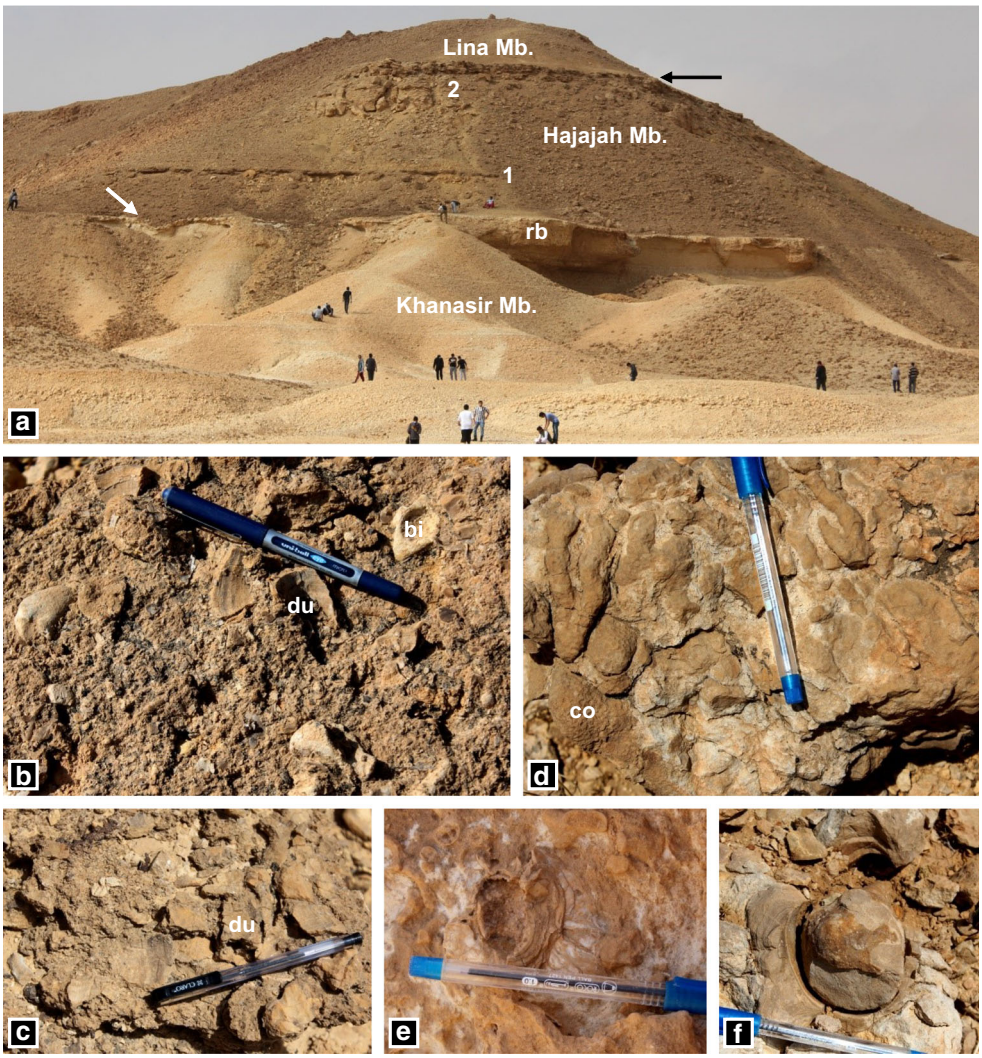

Fig. 4 **a** Aruma Formation outcrop at the Khashm Al Buwaybiyat showing the three successive members. White arrow shows the erosional contact between the Khanasir and Hajajah limestone members. Note the lateral thickness change of the rudist biostrome (rb). The lower and upper limestones are indicated by 1 and 2, respectively, and their close-up views are in b to f. Black arrow is the contact between the Hajajah and Lina members. **b, c** Close-up view of the rudist accumulation in the lower limestone (1), *Durania* (du) fragments are abundant, *Biradiolites* (bi). **d** Branched and small massive coral (co) colonies in upper limestone (2) of figure a. **e, f** Top view of the radiolitids (probably *Biradiolites*), in growth position, in upper limestone (2) in figure a

(Schlumberger), in the uppermost part of the Khanasir Limestone Member in the studied area. The first species is recorded from the Campanian of Organya, Spain, and the second species is recorded from the Campanian of Algeria, Tunisia, France, and western Pakistan. The first description of the rudist fauna, which includes *Durania* cf. *apula* (Parona), *Durania* sp., and *Apricardia* sp. was presented by El-Asa'ad (1987). A new canaliculated rudist genus, *Eodictyoptychus* (type species *Eodictyoptychus arumaensis*), and *Biradiolites* cf. *aquitanicus* Toucas were described from the rudist biostrome, and a Campanian age was proposed by Skelton and El-Asa'ad (1992). The existence of *Durania cornupastoris* (Des Moulins) in the rudist biostrome was only reported, but not described, by Skelton in Cobban et al. (1991, p. D6) in his detailed description of species from the middle Turonian Greenhorn Limestone in Colorado (USA). El-Asa'ad (1991, p. 153) also mentioned that "The rudistid reefal limestone yields an abundant Campanian rudist fauna; these comprise *Dictyoptychus morgani*, *Durania cornupastoris*, *D. gaensis* and *Biradiolites lumbricalis*" in his study on Late Cretaceous ammonites from central Saudi Arabia. The Campanian age is accepted by El-Nakhal and El-Naggar (1994) and Sharland et al. (2001). Recently, this age was also accepted by Gameil and El-Sorogy (2015) and Al-Kahtany et al. (2016) for the rudist biostrome.

Our rudist specimens were collected from this biostrome, and the Campanian age is here accepted as proposed in the previous studies. We observed that the rudist biostrome is mainly constructed by *Durania cornupastoris*, and it also yields *Biradiolites* sp., *Bournonia* sp., and ?*Dictyoptychus* sp. The well-preserved specimens of *Durania cornupastoris* have recently been described by Özer and El-Sorogy (2017), but the other radiolitids will be discussed separately because transverse sections of the right valves show the precise radial structures related to the radial bands (Pons and Vicens 2008), which differ from those of previous studies.

The lenticular rudist biostrome caps the member and overlies a substratum of bioclastic wackestones to floatstones with abundant dacycladacean algae (*Salpingoporella arumaensis* Okla, *Dissocladella intercedens* Bakalova, *Griphoporella* sp.), larger foraminifers, few gastropod and bivalve molds, and poorly preserved echinoids (Gameil and El-Sorogy 2015; Al-Kahtany et al. 2016). This unit may have provided a suitable substrate on which the rudists grew. Large, very thick, barrel- or cylindroconical-shaped rudists with small attachment base built the biostrome. Scattered individuals were inclined and aggregated forms were in upright position. Our rudist bivalves were of an apparently single generation and embedded in growth position (autochthonous).

The top of the Khanasir Limestone Member is an irregular erosional, very low angle unconformity overlain by the Hajajah Limestone Member (Figs. 3d, 4a) (Skelton and El-Asa'ad 1992; Gameil and El-Sorogy 2015; Al-Kahtany et al. 2016; El-Sorogy et al. 2016). This unconformity is also known in the lower Campanian of Iraq, Kuwait, Bahrain, Qatar, and Abu Dhabi (Sharland et al. 2001), which shows its regional extent on the Arabian plate. The characteristic facies of the Hajajah Limestone Member (El-Sorogy et al. 2016) are composed of the following, in ascending order: (1) green shale, brown-weathering, flaky, which laterally changes into marl and argillaceous limestone with scarce ostracods and foraminifers, and cross-bedded sandstone (~ 16 m); (2) creamy limestone, soft, chalky, and slightly argillaceous with abundant coral and stromatoporoid clasts (~ 5 m), the base of which consists totally of rudist fragment accumulations (30–40 cm) of *Durania*, *Biradiolites*, ?*Bournonia*, *Eodictyoptychus*, and *Dictyoptychus* (Fig. 4a, b, c). No rudists are in life position and the fragments are similar to the rudist fauna of the biostrome that caps the Khanasir Limestone Member; (3) green shale, brown-weathering, flaky with ostracods and foraminifers (~ 30 m) that laterally changes into marl and argillaceous limestone; (4) creamy dolomitized limestone, chalky, massively bedded characterized by abundant branched and small massive corals and stromatoporoids (~ 12 m). A lenticular limestone with radiolitids and sparse canaliculated rudists is present in the uppermost part of the coralline limestone (Fig. 4d–f). The Hajajah Limestone Member does not contain the rudist biostrome.

Although four faunal zones showing Campanian–Maastrichtian age were determined by El-Asa'ad (1983b) in the Hajajah Limestone Member, later, a late Campanian age was proposed due to the presence of ammonites in the calcareous upper part of the member (El-Asa'ad 1991; Skelton and El-Asa'ad 1992). But, one of the faunal zones comprises *Omphalocyclus macroporus* (Lamarck) suggesting a Maastrichtian age (Hardenbol et al. 1998), which contradicts the late Campanian age. However, this larger benthic foraminifer was also reported from the upper Campanian formations of the United Arab Emirates (Morris and Skelton 1995), Apulia, Italy (Schlüter et al. 2008), and southeastern Anatolia, Turkey (Özcan 2007; Steuber et al. 2009).

The Hajajah Limestone Member passes upward into the Lina Shale Member (Fig. 4a), which consists of 10–15-m-thick green shale with gastropods and is overlain by 15–20-m-thick nodular, massive limestones with ammonites, gastropods, and foraminifera of upper Maastrichtian age (El-Asa'ad 1983a). This unit varies in thickness across its lateral extent of about 400 km (El-Asa'ad 1987). It is well-developed at the Khashm Hajajah, Khashm Khanasir, and Khashm Al Buwaibiyat areas, but at Wadi Sahba and Majma'ah, remnants of this unit are capped by an erosional iron-encrusted surface with remnant paleosoil. El-Asa'ad (1983b) determined a single faunal zone in this member: the *Omphalocyclus macroporus*/*Fissoelphidium operculiferum* Assemblage Zone (upper Maastrichtian).

The stratigraphy and the unconformities in the Aruma Formation in the studied area are correlated with those of the Arabian Plate (Sharland et al. 2001): 92 Ma for the "middle Turonian Unconformity," 82 Ma for the "lower Campanian Unconformity," and 63 Ma for the "pre-Cenozoic Unconformity" within the AP9-Arabian Plate tectonostratigraphic megasequence (Fig. 2). However, the ages of Philip et al. (2002) differ greatly; according to these authors, the age of the Aruma Formation is upper Maastrichtian instead of Coniacian–upper Maastrichtian, the Hajajah Limestone Member contains rudist-rich biostromes, which are not observed here, and the Lina Shale Member is not observed in the study area. Furthermore, a Paleocene age is suggested for the Hajajah based on marine vertebrates found in northern Saudi Arabia instead of upper Maastrichtan. We believe that this conflict should be solved by future studies.

Diagenesis

Radiolitid shells are mainly composed of two layers, a calcitic outer shell layer consisting of fibrous prisms of low-Mg calcite and an originally aragonitic inner shell layer (Skelton 1974). The outer shell layer seems to be more stable and well-preserved original microstructure than the inner shell layer, which generally is altered to calcite. The original highly porous cellulosprismatic structure of the outer shell layer is currently considered a very important diagnostic feature for taxonomy and phylogeny of the Radolitidae, but it presents also valuable data here to understand the diagenesis of these quite unique fossil shells. Its outer shell layer is mostly thick than other rudists, commonly formed by growth lamellae showing compact or non-compact structures due to the various styles folding and its development pattern. The compact structure may be formed in the outermost margin of non-compact structure where the destruction of the borings is frequently observed (Pons and Vicens 2008). Diagenetic features can be developed in the cellulosprismatic outer shell layer according to the conditions of environment.

Diagenetic features in the present study are based on petrographic and macroscopic analyses of the loose right valves of *Durania*, *Biradiolites*, and *Bournonia* radiolitids. The studied radiolitid rudist bivalves have underwent cementation and neomorphism, dissolution, micritization, silicification, dolomitization, fragmentation and compaction, and bioerosion as described in the subsequent sections.

Cementation and neomorphism

Isopachous calcite crystals and sparry equant calcite are the main cement types in the radiolitid shells (Fig. 5a–f). However, the micritic calcite cement seems to present in some cells, where the cell walls may be thickened due to micritic cement overgrowth (Fig. 5e–g). Some remnant pores are filled with fine-grained sediment (Fig. 5a–f). The crystal growth of the cements exhibits their peculiar texture and origin. Isopachous calcite crystals and sparry equant calcite cements envelope the calcitic outer shell layers, and fine-grained carbonate sediments occur mostly in the body cavity of the right valves. Low-Mg calcite replaces the aragonitic inner shell layer.

Thin isopachous dog-tooth spar fringes of calcite surround cell walls (Fig. 5c). These fringes may be up to three quarters of the cell wall thickness in some places. Calcite cement crystals are approximately 30 to 40 μm long and 5 to 10 μm wide. Similar features are also observed in rudist valves at Abu Roash, Egypt (Mansour 2004). The sparry equant calcite cements are medium to coarse, subhedral crystals, without a preferred orientation, entirely or partially filling the rudist cells (Fig. 5a–f), and consequently plug and reduce different types of porosity, especially vuggy types. Smaller-sized crystals (microspars) are at margins, and they become coarse toward the pore center (Fig. 5a, b).

The body cavities of the radiolitids are entirely or partially filled by fine-grained carbonate deposits consisting of peloidal grains, benthic foraminifera, rudist, and indeterminate shell fragments (Figs. 5h, 9g). These internal sediments are considered syndepositional. XRD analysis shows that calcite is most common in these deposits, constituting the major mineral in the *Durania* and *Biradiolites* specimens. Anorthite and hematite are trace minerals ($2\theta = 33.25$) in *Durania*, and hematite are minor minerals in *Biradiolites* (Figs. 7, 8).

Dissolution

The inner shell layer is more commonly dissolved than the outer shell layers of our radiolitid right valves as described by many studies (Skelton 1974; Al-Aasm and Veizer 1986a, b; Alsharhan 1995; Sanders 2001; Scholle and Ulmer-Scholle 2003; Pascual-Cebrıan et al, 2016). But, there are significant differences in the diagenesis of former aragonitic and calcitic parts of the shell: the inner shell layers have been altered by dissolution and subsequent precipitation of calcite spar or sediments. The texture of the calcitic outer shell layer is more preserved than the inner shell layer such that the cellular prismatic structure can be observed in the macroscopic samples and also in thin sections. The skeletal cavities in the calcitic outer shell layer are relic rather than vugs, and in some places the cells are partially filled with yellowish-deposits and partially or entirely with sparry calcite (Figs. 5a–d, 6a–d, 9f). The framework dissolution pores developed in relict rudist cells have been recently studied in the middle Cretaceous Mishrif Formation of Iraq (Jie et al. 2016, Fig. 3a, b) and can be compared with those of observed in this study.

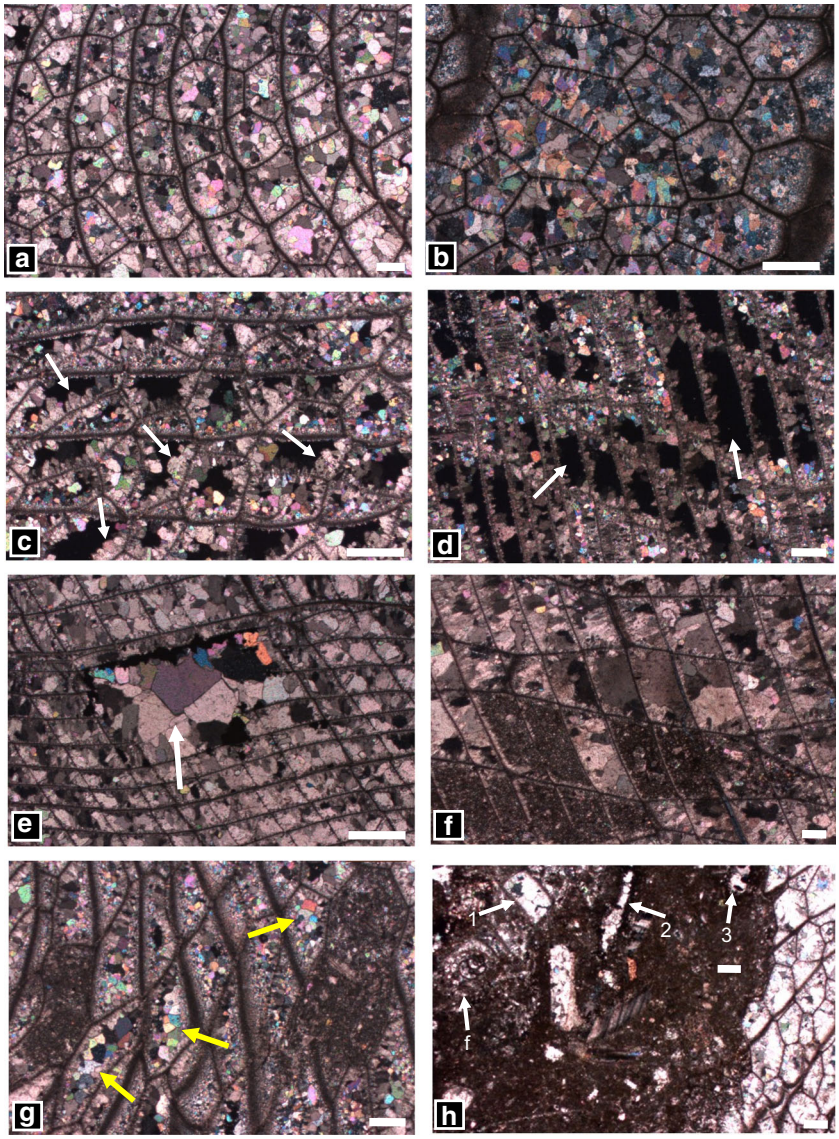

Fig. 5 Cross-polarized photomicrographs. **a, b** *Durania* sp., transverse sections of the outer shell layer showing equant calcite cement entirely or partially filling the outer shell layer cells. Crystal size coarsens from margins toward center of cavity as per available accommodation space, Nos: MGD-CSc-KSU 14 and 16. **c** *Durania* sp., transverse section of the outer shell layer, thin isopachous dog-tooth calcite spar fringes of the cell wall (white arrows), No: MGD-CSc-KSU 27. **d** *Biradiolites* sp., radial section of the outer shell layer showing empty cavities (white arrows), which may enhance porosity, No: MGD-CSc-KSU 57. **e** *Biradiolites* sp., tangential section of the outer shell layer, collapse of body cells and filled with blocky calcite cement (white arrow), No: MGD-CSc-KSU 59. **f** *Bournonia* sp., tangential section of the outer shell layer, spary equant calcite cement and fine-grained carbonate sediments entirely or partially filled the cells, No: MGD-CSc-KSU 48. **g** *Durania* sp., transverse section of the outer shell layer with elongated polygonal cells. Note that the quartz crystals (yellow arrows) and the micritic calcite cement in the cell walls may be thickened due to micritic cement overgrowth, No: MGD-CSc-KSU 18. **h** *Durania* sp., transverse section of the body cavity; it is approximately filled with carbonate sediments, including fine shell fragments (formerly aragonite replaced by fine- to medium-crystalline calcite), benthonic foraminifera (f white arrow) and peloidal grains. Note the three types of micrite envelopes (1-2-3: white arrows, see text for further information), No: MGD-CSc-KSU 32. Scale bars indicate 0.5 mm

Three types of porosity—vuggy, moldic, and enlarged intergranular porosity—form by dissolution. Vuggy and moldic porosity are the main dissolution types observed in rudist shells embedded in platform-type carbonates. The empty cavities may have enhanced the porosity capacity of the rudist biostrome (Choquette and Pray 1970;Bathurst, 1975; Tucker and Wright 1990; Mutti, 1995; Ross and Skelton 1993; Moss and Tucker 1995; Moore 1997; Selley, 2000; Sanders 2001; Tibljaš et al, 2004; Taghavi et al, 2006; Flügel 2010 Enos et al, 2015; Du et al, 2015). However, intraskeletal porosity seems to be very characteristic and is common in the rudist biostrome. Body cavities that are partially filled with sediments, which are exposed now by weathering, indicate an original intraskeletal porosity in the radiolitid specimens

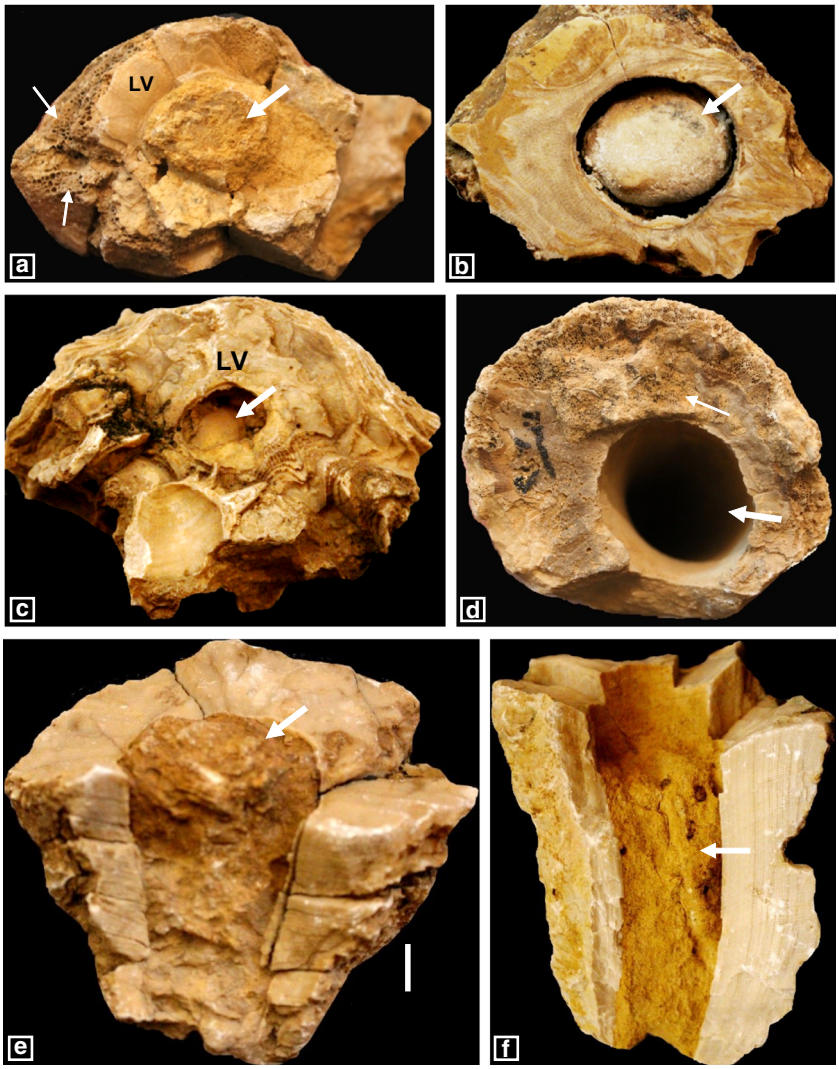

Fig. 6 **a-f** Body cavities are collapsed entirely or partially filled with yellow or yellowish-gray fine grained deposits (thick white arrows). Note the body cavities provided an original intraskeletal porosity. Some parts of the cellular outer shell layer are filled with yellowish deposits (thin white arrows). The left valve (LV) can be partially preserved in a and c. **a, c, d** Natural transverse views of the right valve. **b** Transverse section of the right valve. **e, f** Natural longitudinal sections of the right valve. **a** *Biradiolites* sp., No: MGD-CSc-KSU 56. **b** *Bournonia* sp., No: MGD-CSc-KSU 49. **c** *Bournonia* sp., No: MGD-CSc-KSU 51. **d, e, f** *Durania* sp. **d** No: MGD-CSc-KSU 19. **e** No: MGD-CSc-KSU 33. **f** No: MGD-CSc-KSU 30. Scale bar indicates 10 mm

(Fig. 6b–f). This is common in the platform-type carbonates of the Periadriatic Domain, Italy (Cestari and Sartorio 1995) and NW Jordan (Özer and Ahmad 2016).

Micritization

Micritic envelopes are mainly observed around benthic foraminifera, rudist, and indeterminate shell fragments in the fine carbonate sediments filling the body cavities (Fig. 5h). Three types of micritic envelopes surround the components of the matrix: the first is very thin, the second is intensely developed and has destroyed approximately a major portion of the clast, and the third consists of bored holes in-filled with micrite and micritic envelops (Fig. 5h). Similar micritic envelopes are commonly determined in the rudist components of the limestones (Longman 1980; Jordan et al. 1985; Cestari and Sartorio 1995; Sanders 2001; Flügel 2010; Asghari and Adabi 2014).

In general, the outline and morphology of the radiolitid cells are preserved; however, the thickening of some cell walls may be observed as explained previously.

Silicification

Silicification is the secondary filling of pore spaces with fine-grained quartz, chalcedony, or opal. It may partially affect the calcitic outer shell layer and even fill the body cavity of radiolitids (Fig. 9a–d). HCl tests on the outer shell layer of the valve show the preservation of its original calcitic structure. XRD analysis of the deposits filling the body cavity also presents very limited evidence of silicification (Figs. 7, 8). Silica is a minor element in *Durania* specimens, and it is a trace mineral ($2\theta = 26.65$) in *Biradiolites* specimens.

Fine fibrous chalcedony pore-filling with equigranular megaquartz partially replaces calcitic parts of the shell structures (Fig. 9a–d). Although the processes of dissolution are

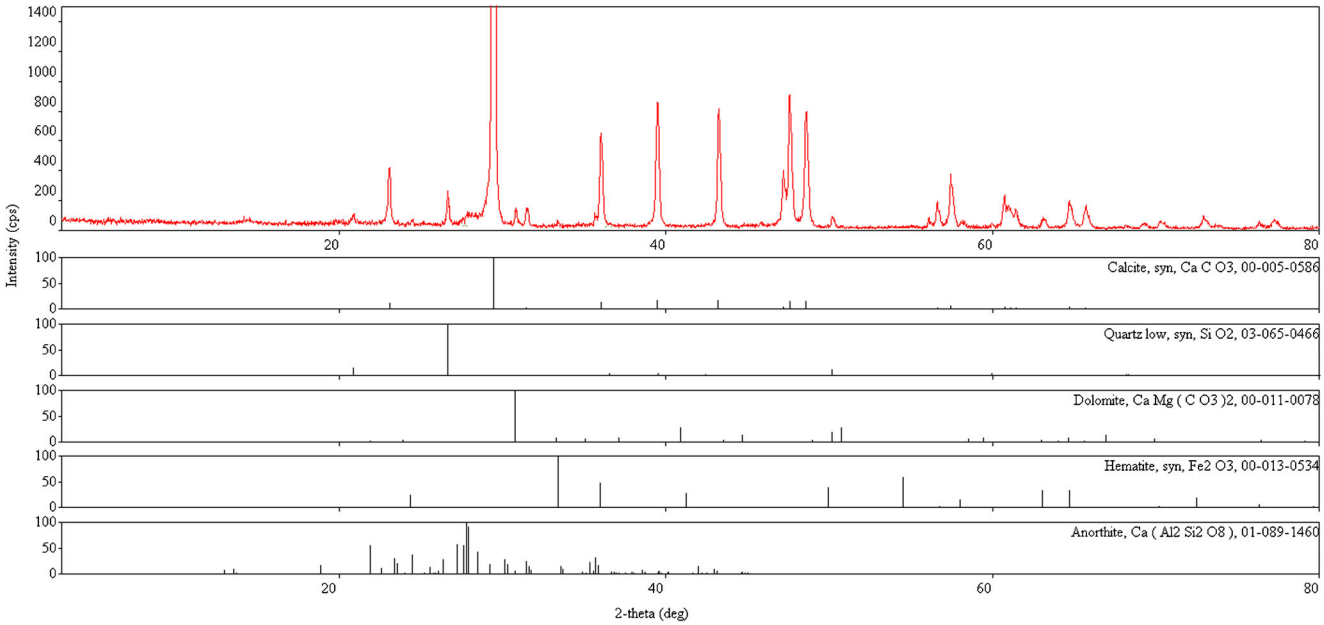

Fig. 7 XRD pattern of the sample from the fine-grained yellowish deposits of body cavity of *Durania* sp.; specimen no: MGD-CSc-KSU

still uncertain, it is apparent that silicification occurred during and/or after dissolution, as has been explained in many studies (Jacka 1974; Knauth 1979; Schmitt and Boyd 1981; Holdaway and Clayton 1982; Lawrence 1994).

Authigenic silica is commonly observed as chalcedony filling cells of the outer shell layer of radiolitids (Fig. 9a–d). Authigenic equigranular megaquartz is rare partially filling the shell structures (Fig. 9c). Coarse to medium, equigranular megaquartz partially fills cells and is in sharp contact with the walls of the cell (Fig. 9d). Some walls have been replaced by silica; however, they were not dissolved, and so, the original cellular structure is preserved. Small spherulitic shapes and wavy extension in crystals show finely fibrous fabric. In general, chalcedony is usually destructive to the cellular structure of the valve, but the remains of primary calcite can be preserved in chalcedony crystals. Silicification crosscuts also all other diagenetic phases of the shells (Fig. 9a, c).

Data on silicification of rudists is limited and mainly based on microfacies studies of fragments (Braun and Hirsch 1994; Philip and Platel 1995; Sanders 1998; Mansour 2004). This process was recently discussed on completely silicified-free

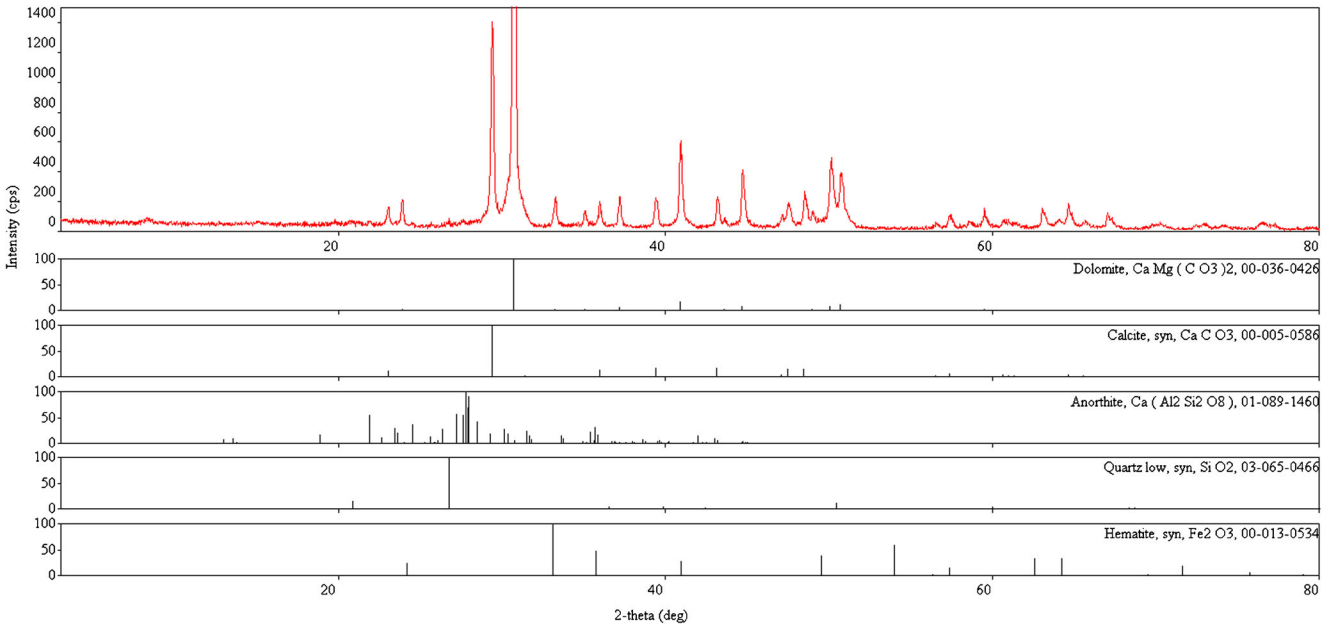

Fig. 8 XRD pattern of the sample from the fine-grained yellowish deposits of body cavity of *Biradiolites* sp.; specimen no: MGD-CSc-KSU 56

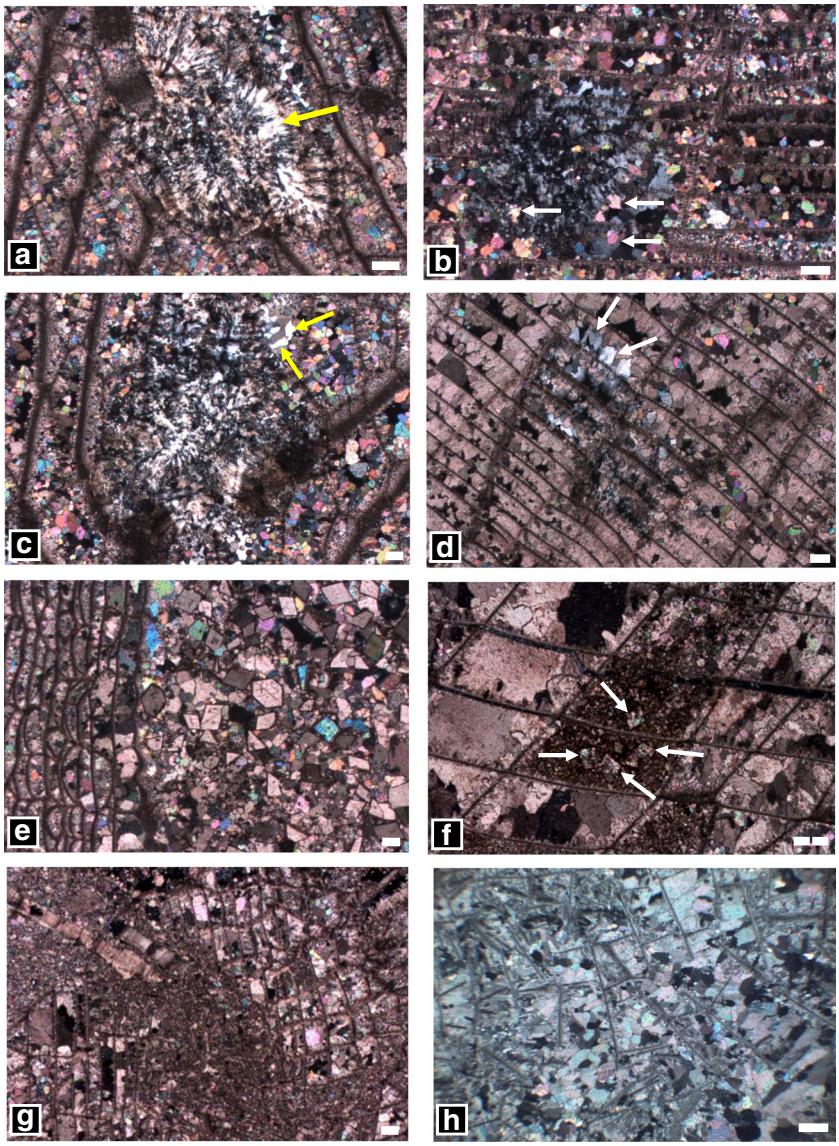

Fig. 9 Cross-polarized photomicrographs. **a-c** *Durania* sp., transverse sections of the outer shell layer. Note the destruction of the cells and the cross-cutting of all other diagenetic phases by silicification. **a** The finely fibrous chalcedony pore-filling with equigranular megaquartz (yellow arrow), No: MGD-CSc-KSU 26. **b** The spherulitic pore-filling chalcedony with relics of the original calcitic components (white arrows), No: MGD-CSc-KSU 22. **c** The finely fibrous chalcedony pore-filling with equigranular megaquartz (yellow arrows). Note the silicification cross-cutting all other diagenetic phases of the shell, No: MGD-CSc-KSU 28. **d** *Biradiolites* sp., radial section of the outer shell layer, the coarse- to medium-equigranular megaquartz and their sharp contact with the walls of the cell (white arrows). Note some cell walls destroyed by silica; however, they are not dissolved and so the original cellular structure is preserved, No: MGD-CSc-KSU 58. **e** *Biradiolite*s sp., transverse section of outer shell layer and body cavity. Euhedral to subhedral dolomite crystals replace calcite in the body cavity. The cellular layer filled with secondary calcite, No: MGD-CSc-KSU 60. **f** *Bournonia* sp., transverse section of the outer shell layer, the sparry equant calcite cement, and fine-grained carbonate sediments entirely or partially filled the cells. A few dolomite rhombs with cloudy appearance can be observed in the deposits filling the cells (white arrows), No: MGD-CSc-KSU 52. **g** *Bournonia* sp., transverse section of the body cavity showing the fragments of the outer shell layer within the fine debris, No: MGD-CSc-KSU 54. **h** *Bournonia* sp., transverse section of the outer shell layer showing the breaking up of the cell walls of the outer shell layer, No: MGD-CSc-KSU 53. Scale bars indicate 0.5 mm

specimens of the upper Cenomanian canaliculated rudists and *Sauvagesia* in northwestern Jordan (Özer and Ahmad 2016) and on embedded silicified specimens in western Algeria (Benyoucef et al. 2016).

Many sources of silica are possible: silica can be produced by dissolution of siliceous organisms, sand and silt quartz grains or feldspar, chert nodules in limestone, volcanic ash, or by local hydrothermal activity, and by transformation of montmorillinite to illite or mica (Jacka 1974; Keene and Kastner 1974; Knauth 1979; Maliva and Sıever 1988). Accordingly, the source of silica for silicification of these rudists may have come from underlying siliciclastic rocks in the Wasia Formation (quartz, feldspar, and clay minerals), from dolomitic limestone in the Khanasir Limestone

Member or from surrounding Upper Cretaceous carbonate rocks. Presence of chalcedony sphaerulites with a wavy extinction and finely fibrous structure suggest that at least a part of the silica may derive from former evaporates, which can be probably developed very restricted.

Dolomitization

Sparse euhedral to subhedral dolomite crystals are disseminated in the fine-grained matrix of body cavities and in the internal sediments that fill some of the cells of the outer shell layer (Fig. 9e, f). The dolomite crystals have partially (*Durania* and *Bournonia* specimens) or entirely (*Biradiolites* specimens) invaded the body cavity and replaced fine carbonate-fill deposits (Fig. 9e). XRD analysis shows that dolomite crystals were more pervasive in body cavity fill of *Biradiolites* specimens than of *Durania* (Figs. 7, 8). Hence, dolomite is common in *Biradiolites* specimens, while it is minor in *Durania*.

Some dolomite rhombs are zoned with cloudy centers and clear rims. The cloudy appearance may result from high amounts of inclusions as explained by Shakeri (2013) and Asghari and Adabi (2014). A few dolomite rhombs with cloudy appearances fill cells of the outer shell layer (Fig. 9f).

Fragmentation and compaction

Most radiolitid valves in our study have been broken presumably by storms, currents, and/or winnowing, and the fragmentation seems to have been more common than by compaction. The horizontal and vertical fractures are mostly observed in radiolitid valves, but diagonal fractures are locally present (Fig. 10a–f).

In our study area, radiolitids were mostly in vertical to inclined growth position. Some radiolitid specimens (*Durania* especially) have been broken and show only their radial bands due to the fact that the shell is thinner in the furrows delimiting the radial bands so that shells will have preferentially broken along these furrows during reworking or compaction (Fig. 10a–f). Coarse and fine rudist debris is also present in the fine carbonate sediment filling the body cavities of the right valves (Fig. 5h). Breakage of the cell walls probably occurred before deposition of the equant calcite cement (Fig. 9h).

The original cell structures of the outer shell layers have been destroyed and exposed to silicification where the fibrous chalcedony can be observed in our specimens (Fig. 9a–c).

The compaction of rudist valves has been reported by many studies and compares with our specimens (Halley 1985; Alsharhan 1995; Moss and Tucker 1995; Sanders 1998, 2001; Alsharhan and Sadd 2000; Mansour 2004; Shakeri 2013; Asghari and Adabi 2014).

Bioerosion

Bioerosion is the most characteristic and abundant feature in our radiolitid right valves. The well-preserved valves show few small holes in the uppermost parts of the valve, whereas fragments of the valve are characterized by intense large borings affecting previously precipitated cement in some rudist shells (Fig. 10a–f). The latter may indicate that the radiolitid fragments were on the sea floor for a long post-mortem period. The small holes were probably bored by algae and fungi; the large ones by clionid sponges. Three types of borings can be distinguished (Fig. 10a, b, c, d, e): (1) the first consists mostly of the ovoid holes with diameters ranging in size between 2 × 3 mm and 8 × 10 mm. They are either void or partially filled with sediments. The larger holes extend through the thick shell wall. (2) The second group of borings is about 1 mm or less in length, having irregular shape and filled with gray, fine-grained sediments, and (3) smaller, rounded borings, 50–60 μm in diameter filled with gray, fine-grained sediment. The first two types can be observed in the same specimen (Fig. 10a–c).

Borings in rudist shells like our specimens are well represented in many rudist-bearing limestones (Aqrawi et al. 1998; Moss and Tucker 1995; Alsharhan 1995; Sanders 1998, 2001; Sanders and Pons 1999; Alsharhan and Sadd 2000; El-Hedeny and El-Sabbagh 2005; Strohmenger et al. 2006; Shakeri 2013).

Interpretations and discussion

Loose specimens of radiolitids from the lenticular rudist biostrome in the uppermost part of the Khanasir Limestone Member have underwent diagenetic features, such as cementation, neomorphism, dissolution, micritization, silicification, dolomitization, fragmentation, and compaction and bioerosion. The nodular limestones below the rudist biostrome in the lithological sequence of the Khanasir Limestone Member are algal wackestone, foraminiferal algal wackestone, and algal packstone with abundant dasycladacean algae, and all bioclastic fragments are recrystallized (Al-Kahtany et al. 2016). New petrographic studies show the presence of sparry calcite cement, neomorphic features, micritic envelopes around bioclasts, dissolution of the fragments, dolomitization with associated vuggy porosity, silicification, and bioerosional features. These data indicate that the nodular limestones of the Khanasir Limestone Member were also affected by the same diagenetic alterations as the radiolitids in the overlying rudist biostrome.

Although most of the diagenetic features indicate a marine diagenetic environment, there are very limited data on the presence of the meteoric environments, which are presented and discussed subsequently:

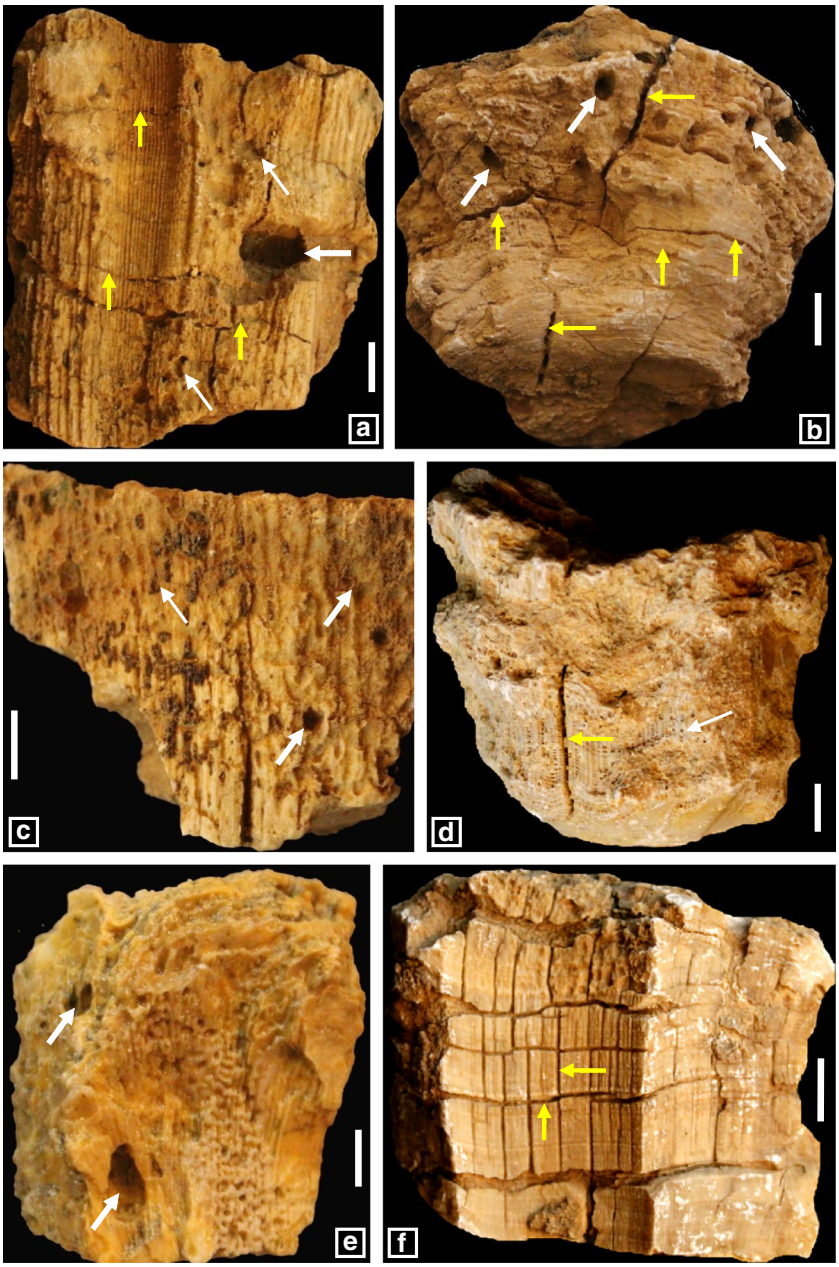

Fig. 10 **a–f** *Durania* sp. Note the intense fracturing and bioerosion of incomplete valves. Yellow arrows indicate fracturing, thick white arrows show large borings, and thin white arrows point to small borings. Scale bar indicates 10 mm. Sample nos of a–f MGD-CSc-KSU 25, MGD-CSc-KSU 35, MGD-CSc-KSU 37, MGD-CSc-KSU 28, MGD-CSc-KSU 40, MGD-CSc-KSU 29

Fragmentation, bioerosion and micritization are the main diagenetic events developed in the marine diagenetic environment. Marine calcitic cement seems to be pericipitated along the cell walls during this environment (probably an early marine diagenetic stage).

The valves were mainly fragmented due to winnowing and currents or storms. However, the effect of bioerosion by algal, fungal, and clinoid sponge borings also may have enhanced valve breakage. Valve fragments are found in the rudist biostrome level and also body cavities. The inclined valves below erect individuals in life position and the fragmented, fractured, and breakage of the cell walls indicate that the rudist valves suffered mechanical forces due to high-energy physical conditions in a marine environment. The large and small borings indicate intense marine bioerosion. It can be seen that bioerosion affects previously precipitated cement in some rudist shells during the early marine diagenetic stage. The large borings of the valves may indicate that the radiolitid fragments were on the sea floor for a long post-mortem period.

Micrite envelopes were developed around the grains during an early marine diagenetic phase in limestones as emphasized in many studies (Longman 1980; Jordan et al. 1985; Scoffin 1987; Nizami and Sheikh 2009; Sahraeyan et al. 2013).

The fact that the studied levels are overlain by regional unconformities, for example, the top of the rudist biostrome

was exposed at the unconformity between the Khanasir Limestone Member and the Hajajah Member, and also a disconformity was formed between the Lina Shale Member and the Umm er Radhuma Formation. They are most probably linked to episodes of subaerial exposure, which may have resulted in diagenetic features characteristic of the vadose zone. Silicification and dolomitization are the main important diagenetic processes in this environment. Also, the isopachous and sparry calcite cement and neomorphism are characteristic features of this zone. However, they are very limited observed in the studied radiolitid shells. It shows that the meteoric diagenetic environments were developed relatively short times, and it is very probably in arid climates where diagenetic alteration may be limited than humid climates.

The presence of silicification which crosscuts all other diagenetic phases of the shells supports this interpretation due to silica-saturated waters and low pH conditions that were occasionally developed in the environment resulting in authigenic silica pore-fill and silicification that may have occurred very recently, after subaerial exposure of the shells. This is a very common process in arid environments. The absence of the chemical solutions in the radiolitid shells may also support the very limited silicification effects in the environment probably due to arid climates. Silicification could also be a recent process whereby the silica is derived from wind-blown quartz, a process common in arid environments. The chalcedony sphaerulites with a wavy extinction and finely fibrous structure may postulate the interruption of normal marine conditions in an arid context prone to generate evaporates. Dolomite crystals are sparse in the fine-grained matrix of body cavities and in the internal sediments filling the cells of the outer shell layer. There is thus evidence that the internal sediments filling either the body chamber or parts of the outer shell are partially dolomitized, but no evidence about the dolomitization of the actual shell. However, it suggests the presence of the development of dolomitization conditions in environment, but very limited probably due to arid climates.

Aragonite is unstable in meteoric waters; so, the aragonitic inner shell layer of the valves and aragonitic grains were totally dissolved in this setting.

Isopachous and equant calcite are uniformly distributed in the cells of the outer shell layer. Isopachous calcite cement encrusts and occludes prismatic cells in the walls. Although, the development of thin isopachous calcite dog-tooth spars seems to suggest freshwater phreatic influence (Longman 1980; James and Choquette 1984; Tucker 1988; Moss and Tucker 1995; Scholle and Ulmer-Scholle 2003) or probably linked early meteoric diagenetic cement as indicated by Vandeginste et al. (2013) and Loucks et al. (2013), this is not necessarily the case (e.g. Flügel 2010). The coarsening of the equant calcite toward pore center may indicate freshwater pharetic zone.

The sediment infill of parts of the originally hollow structure of the outer shell layer can be observed, but they could have occurred much earlier, possibly even during the life of the bivalves.

Conclusions

The Aruma Formation overlies the continental clastics of the Cenomanian Wasia Formation in central Saudi Arabia and is composed of three members, from base to top, the Coniacian to Campanian Khanasir Limestone Member, the late Campanian Hajajah Limestone Member, and the late Maastrichtian Lina Shale Member. Two major unconformities were recorded within the Aruma Formation, the "lower Campanian unconformity" between the Khanasir Limestone Member and the Hajajah Limestone Member and "the pre-Cenozoic unconformity" between the Lina Shale Member and Paleogene Umm er Radhuma Formation.

Petrographic and macroscopic studies of the loose radiolitids collected from a lenticular rudist biostrome in the uppermost part of the Khanasir Limestone Member showed the diagenetic processes, such as cementation and neomorphism, dissolution, micritization, silicification, dolomitization, fragmentation and compaction, and bioerosion, which are summarized in the subsequent texts.

Marine calcitic cement is limited observed, while isopachous dog-tooth spar cement fringes many rudist outer walls and sparry equant calcite fills cell interiors. Body cavities of the right valves are entirely or partially filled by fine-grained carbonate sediment. The cells of the prismatic outer shell layer are partially or entirely filled with sparry calcite and sediment, consequently plugging or reducing the porosity of the specimens. Original aragonitic inner shell layer and aragonitic allochems were dissolved and molds infilled by more stable diagenetic calcite or sediments. Micritic envelopes commonly surround fragments in the sediments and fill body cavities.

Silicification of megaquartz, fibrous chalcedony, or opal partially affects the outer shell layer. Sparse euhedral to subhedral dolomite crystals are disseminated in the fine-grained matrix of body cavities and in the internal sediments that fill some of the cells of the outer shell layer. Many shells have been flattened and broken by high energy currents. Small, irregular, and large borings by algae, fungi, and clionid sponges are abundant in the well-preserved valves and in their fragments.

The recorded diagenetic alterations indicate that they occurred essentially under marine environment; however, meteoric diagenetic environments with arid climates and fresh water pharetic zone may be also developed due to subaerial exposures of unconformities.

Acknowledgments The authors would like to extend their sincere appreciation to the Deanship of Scientific Research at the King Saud University for funding this work through research group no. (RG-1438-060). We thank Dr. Hatice Yılmaz (Dokuz Eylul University, İzmir) for XRD analysis and interpretations; Winton Cornell (The University of Tulsa) for comments on XRD analysis; Ibukun Bode-Omoleye (Oklahoma State University) for English corrections of the text; and Dr. Cüneyt Akal and Dr. Toygar Akar from the Dokuz Eylul University, İzmir, for formatting the figures. The authors would like to thank Dr. Robert W. Scott (The University of Tulsa) for his constructive suggestions and English corrections of the text and to two anonymous reviewers that improved the quality of the study. We are also grateful to Dr. Bruno Granier (Université de Bretagne Occidentale, Brest) for his valuable comments on the text.

References

Al-Aasm IS, Veizer J (1986a) Diagenetic stabilization of aragonite and low-Mg calcite; I, stable isotops in rudists. J Sediment Petrol 56: 138–152

Al-Aasm IS, Veizer J (1986b) Diagenetic stabilization of aragonite and low-Mg calcite; II, trace elements in rudists. J Sediment Petrol 56: 763–770

Al-Kahtany K, El-Sorogy AS, Youssef M (2016) Stratigraphy and depositional environments of the Upper Cretaceous Aruma Formation, Central Saudi Arabia. Arab J Geosci 9:330–339

Al-Mohammad RAH (2012) Depositional environment and petrophysical properties study of Mishrif Formation in Tuba Oilfield, Southern Iraq. J Basrah Res (Sci) 38(1):25–50

Alsharhan AS (1995) Facies variation, diagenesis, and exploration potential of the Cretaceous rudist-bearing carbonates of the Arabian Gulf. AAPG Bull 79(4):531–550

Alsharhan AS, Nairn AEM (1990) A review of the Cretaceous formations in the Arabian Peninsula and Gulf: part II. Mid Cretaceous (Wasia Group) stratigraphy and paleogeography. J Pet Geol 11:89–112

Alsharhan AS, Sadd JL (2000) Stylolites in Lower Cretaceous carbonate reservoirs, UAE. In: Alsharhan AS, Scott RW (eds) Middle East models of Jurassic/Cretaceous carbonate systems. SEPM Special Publication 69:179–200

Aqrawi AAM, Tehni GA, Sherwani GH, Kareem BMA (1998) Mid-Cretaceous rudist-bearing carbonates of the Mishrif Formation; an important reservoir sequence in the Mesopotamian Basin, Iraq. J Pet Geol 1(1):57–82

Asghari M, Adabi MH (2014) Diagenesis and geochemistry of the Sarvak Formation in Ahvaz oil field-Iran. Geochem J 1(1):1–7

Bandel K, Salameh E (2013) Geologic development of Jordan. Evolution of its rocks and life. The University of Jordan Press, Amman 278 p

Bathurst RGC (1975) Carbonate sediments and their diagenesis. Elsevier Science, New York 658 p

Benyoucef M, Meıster C, Mebarkı K, Läng É, Adacı M, Cavin L, Malti FZ, Zaoui D, Cherif A, Bensalah M (2016) Évolution lithostratigraphique, paléoenvironnementale et séquentielle du Cénomanien-Turonien inférieur dans la région du Guir (Ouest algérien). Carnets Geol 16(9):271–295

Braun M, Hirsch F (1994) Mid Cretaceous (Albian-Cenomanian) carbonate platforms in Israel. Cuad Geol ibér 18:59–81

Cestari R, Sartorio D (1995) Rudists and facies of the periadriatic domain. Agip, Rome 207 p

Chikhi-Aouimeur F (2010) L'Algerié a travers son Patrimoine paléontologique. Les Rudistes. SarlBaosem, Arzew 269p

Choquette PW, Pray LC (1970) Geologic nomenclature and classification of porosity in sedimentary carbonates. AAPG Bull 54:207–250

Cobban WA, Skelton PW, Kennedy WJ (1991) Occurrence of the rudistid *Durania cornupastoris* (Des Moulins, 1826) in the Upper Cretaceous Greenhorn Limestone in Colorado. U S Geol Surv Bull 1985:D1–D8

Du Y, Zhang J, Zheng S, Xin J, Chen J, Li YZ (2015) The rudist buildup depositional model, reservoir architecture and development strategy of the cretaceous Sarvak formation of Southwest Iran. Petroleum 1: 16–26

El-Asa'ad, GMA (1977) A contribution to the geology of the Aruma Formation in Central Saudi Arabia. Ph.D. thesis, Mansoura University, Egypt (Unpublished).

El-Asa'ad, GMA (1983a) Lithostratigraphy of the Aruma Formation in Central Saudi Arabia. Proceeding of the first Jordanian Geological Conference, Special Publication 1:72–86

El-Asa'ad, GMA (1983b) Bio- and chronostratigraphy of the Aruma Formation in Central Saudi Arabia. Proceeding of the first Jordanian Geological Conference, Special Publication 1:87–111

El-Asa'ad GMA (1987) Rudist faunas from the Late Cretaceous of Central Saudi Arabia. J Coll Sci King Saud Univ 18(1):53–71

El-Asa'ad GMA (1991) Late Cretaceous Ammonites from Central Saudi Arabia. J King Saud Univ 3:135–158

El-Hedeny MM, El-Sabbagh AM (2005) *Eoradiolites liratus* (Bivalvia, Radiolitidae) from the Upper Cenomanian Galala Formation at Saint Paul, Eastern Desert (Egypt). Cretac Res 26:551–566

El-Nakhal HA, El-Naggar ZR (1994) Review of the biostratigraphy of the Aruma Group (Upper Cretaceous) in the Arabian Peninsula and surrounding regions. Cretac Res 15(4):401–416

El-Sorogy AS, Ismail A, Youssef M, Nour H (2016) Facies development and paleoenvironment of the Hajajah Limestone Member, Aruma Formation, central Saudi Arabia. J Afr Earth Sci 124:355–364

Enos P (1986) Diagenesis of mid-Cretaceous rudist reefs, Valles Platform, Mexico. In: Schroeder JH, Purser BH (eds) Reef diagenesis. Springer, Berlin, pp 160–185

Enos P, Wahap A, Goldstein R (2015) Diagenesis and porosity evolution associated with unconformities in the mid-Cretaceous El Abra Limestone, Mexico. Kansas Interdisciplinary Carbonate Consortium Prospectus, pp 140–143.

Flügel E (2010) Microfacies of carbonate rocks: analysis, interpretation and application. Springer-Verlag, Berlin, p 929

Gameil M, El-Sorogy AS (2015) Gastropods from the Campanian–Maastrichtian Aruma Formation, Central Saudi Arabia. J Afr Earth Sci 103:128–139

Ghanem H, Kuss J (2013) Stratigraphic control of the Aptiane Early Turonian sequences of the Levant Platform, Coastal Range, northwest Syria. GeoArabia 18(4):85–132

Hajıkazemi E, Al-Aasm IS, Coniglio M (2010) Subaerial exposure and meteoric diagenesis of the Cenomanian-Turonian Upper Sarvak Formation, southwestern Iran. In: Leturmy P, Robın C (eds) Tectonic and stratigraphic evolution of Zagros and Makran during the Mesozoic-Senozoic, vol 330. Geological Society, London, special publication, pp 253–272

Halley RB (1985) Setting and geologic summary of the Lower Cretaceous, Sunniland field, Sothern Florida. In: Roehl PO, Choquette PW (eds) Carbonate petroleum reservoirs. Springer-Verlag, New York, pp 443–454

Hardenbol J, Thierry J, Farley MB, Jacquin T, de Graciansky PC, Vail PR (1998) Cretaceous biochronostratigraphy. In: de Graciansky PC, Hardenbol J, Jacquin T, Vail PR (eds) Mesozoic and Cenozoic sequence stratigraphy of European basins, vol 60. Society for Sedimentary Geology (SEPM), Tulsa, Special Publication, pp 3–13

Harris PM, Frost, SH, Seglie, GA, Schneidermann N (1984) Regional unconformities and depositional cycles, Cretaceous Arabian Peninsula. In: Schlee JS (ed). Interregional unconformities and hydrocarbon accumulation. AAPG Memoire 36, pp 67–80

Holdaway HK, Clayton CJ (1982) Preservation of shell microstructure in silicified brachiopods from the Upper Cretaceous Wilmington Sands of Devon. Geol Mag 119:371–382

Jacka AD (1974) Replacement of fossils by length-slow chalcedony and associated dolomitization. J Sediment Petrol 44:421–427

James NP, Choquette PW (1984) Diagenesis 9. Limestones—the meteoric diagenetic environment. Geosci Can 1(1):161–194

Jie Z, Limin Z, Fuliang LV, Haiying H, Dongxu W, Tianxiang D (2016) Rudists reservoir characterization in Middle Cretaceous Mishrif Formation of H Oilfield, Iraq. Extented abstract AAPG/SEG International Conference & Exhibition, Melbourne, Australia, September 13–16, 2015, AAPG/SEG © 2016.

Jordan CF, Connally RC, Vest HA (1985) Middle Cretaceous carbonate of Mishrif Formation, Fateh Field, offshore Dubai, UAE. In: Roehl PO, Choquette PW (eds) Carbonate petroleum reservoirs. Springer-Verlag, New York, pp 425–442

Keene JB, Kastner M (1974) Clays and formation of deep-sea chert. Nature 249:754–755

Khazaei AR, Skelton PW, Yazdi M (2010) Maastrichtian rudist fauna from Tarbar Formation (Zagros Region, SW Iran): preliminary observations. In: Özer S, Sari B, Skelton PW (eds) Jurassic-Cretaceous rudists and carbonate platforms. Turk J Earth Sci 19(6):703–719

Knauth LP (1979) A model for the origin of chert in limestone. Geology 7:274–277

Lawrence MJF (1994) Conceptual model for early diagenetic chert and dolomite, Amuri Limestone Group, north-eastern South Island, New Zealand. Sedimentology 41:479–498

Longman MW (1980) Carbonate diagenesis textures from near surface diagenetic environments. Am Assoc Pet Geol Bull 64:461–487

Loucks RG, Lucia FJ, Waite LE (2013) Origin and description of the micropore network within the Lower Cretaceous Stuart City trend tight-gas limestone reservoir in Pawnee Field in South Texas. Gulf Coast Assoc Geol Soc 2:29–41

M'Rabet A, Negra MH, Purser BH, Sassi S, Ben Ayed N (1986) Micrite diagenesis in senonian rudist build-ups in Central Tunisia. Reef Diagenesis, pp 210–223

Maliva RG, Sıever R (1988) Mechanism and controls of silification of fossils in limestone. J Geol 96(4):387–398

Mansour ASM (2004) Diagenesis of Upper Cretaceous rudist bivalves, Abu Roash Area, Egypt: a petrographic study. Geol Croat 57(1):55–66

Moore CH (1997) Carbonate diagenesis and porosity. In: Developments in sedimentology, vol 46. Elsevier Science, Amsterdam 317 p

Morris NJ, Skelton PW (1995) Late Campanian–Maastrichtian rudists from the United Arab Emirates—Oman border region. Bulletin of the British Museum (natural history). Geol Ser 51:277–305

Moss S, Tucker ME (1995) Diagenesis of Barremian–Aptian platform carbonates (the Urgonian Limestone Formation of SE France): near-surface and shallow-burial diagenesis. Sedimentology 42: 853–874

Mutti M (1995) Porosity development and diagenesis in the Orfento Supersequence and its bounding unconformities (Upper Cretaceous, Montagna Della Maiella, Italy). In: Budd DA, Saller AH, Harris PM (eds) Carbonate reservoirs, unconformities and porosity in carbonate strata, vol 63. The American Association of Petroleum Geologists, Tulsa, Memoire, pp 141–158

Negra MH (1984) Paleoenvironnement et diagenese des facies recifaux à Rudistes au Jebel el Kebar, Tunisie central. These de 3 Cycle. Univ. Paris-Sud, Orsay

Negra MH, Purser BH, M'Rabet A (2009) Sedimentation, diagenesis and syntectonic erosion of Upper Cretaceous rudist mounds in Central Tunisia. In: Monty CLV, Bosence DWJ, Brıdges PH, Pratt BR (eds) Carbonate mudmounds: their origin and evolution. Blackwell Science, Hoboken, pp 401–417

Nizami AR, Sheikh RA (2009) Microfacies analysis and diagenetic settings of the Middle Jurassic Samana Suk Formation, Sheikh Budin Hill Section, Marwat Range, Trans Indus Ranges, Pakistan. Geol Bull Punjab Univ 44:69–84

Özcan E (2007) Morphometric analysis of the genus Omphalocyclus from the Late Cretaceous of Turkey: new data on its stratigraphic distribution in Mediterranean Tethys and description of two new taxa. Cretac Res 28:621–641

Özer S (2010) *Dictyoptychus* Douvillé: taxonomic revision, phylogeny and biogeography. In: Özer S, Sar B, Skelton PW (eds) Jurassic-Cretaceous rudists and carbonate platforms. Turkish Journal of Earth Sciences 19(5):583–612

Özer S, Ahmad F (2016) *Caprinula* and *Sauvagesia* rudist faunas (Bivalvia) from the Cenomanian of NW Jordan. Stratigraphy and taxonomy. Cretac Res 58:141–159

Özer S, El-Sorogy AS (2017) New record of *Durania cornupastoris* (rudist, Bivalvia) from the Campanian of the Aruma Formation, Riyadh (Saudi Arabia). Description, geographic and stratigraphic remarks. J Afr Earth Sci 129:380–389

Özer S, Fayez A (2015) Cenomanian-Turonian rudist (bivalvia) lithosomes from NW of Jordan. J Afr Earth Sci 107:119–133

Özer S, Karim KH, Sadiq DM (2013) First determination of rudists (bivalvia) from NE Iraq: systematic palaeontology and palaeobiogeography. Bull Mineral Res Explor 147:31–55

Pascual-Cebrıan E, Götz S, Bover-Arnal T, Skelton PW, Gılı E, Salasand R, Stınnesbeck W (2016) Calcite/aragonite ratio fluctuations in Aptian rudist bivalves: correlation with changing temperatures. Geology 44(2):135–138

Philip J (1982) Paléobiogéographie des rudistes et géodynamiques des marges mésogéennes au Crétacé supérieur. Bull Soc Géol Fr 24(7): 995–1006

Philip J (1985) Sur les relations des marges téthysiennes au Campanien et au Maestrichtien déduits de la distribution des rudistes. Bull Soc Géol Fr 1(8):723–731

Philip J, Platel JP (1995) Stratigraphy and rudist biozonation of the Campanian and Maastrichtian of Eastern Oman. Rev Mex Cienc Geol 12(2):257–266 (for 1995)

Philip J, Roger J, Vaslet D, Cecca F, Gardın S, Memesh AMS (2002) Sequence stratigraphy, biostratigraphy and paleontology of the Maastrichtian-Paleocene Aruma Formation in outcrop in Saudi Arabia. GeoArabia 7(4):699–718

Pons JM, Vicens E (2008) The structure of the outer shell layer in radiolitid rudists, a morphoconstructional approach. Lethaia 41: 219–234

Powers RW (1968) Arabie Saoudite. In: Lexique Stratigraphie Internationali, vol III: Asie, fasc. 10b. Center National de la Recerche Scientifique, Paris 177 p

Powers RW, Ramirez LF, Redmond CD, Elberg EL, Jr (1966) Geology of the Arabian Peninsula. Sedimentary geology of Saudi Arabia. U.S. Geol Surv Prof Paper 560–D, 147 p

Ross DJ, Skelton PW (1993) Rudist formations of the Cretaceous: a palaeoecological, sedimentological and stratigraphical review. In: Wright VP (ed) Sedimentology review, vol 1. Blackwell Scientific Publications, Hoboken, pp 73–91

Saber GS, Salama YF, Scott RW, Abdel-Gawad GI, Aly MF (2009) Cenomanian-Turonian rudist assemblages and sequence stratigraphy on the North Sinai carbonate shelf, Egypt. GeoArabia 14(4): 113–134

Sadooni FN (2005) The nature and origin of Upper Cretaceous basin-margin rudist buildups of the Mesopotamian Basin, southern Iraq, with consideration of possible hydrocarbon stratigraphic entrapment. Cretac Res 26(2):213–224

Sahraeyan M, Bahrami M, Arzaghi S (2013) Facies analysis and depositional environments of the Oligocene-Miocene Asmari Formation, Zagros Basin, Iran, southwestern Iran. J Geosci Front:1–10

Sanders D (1998) Upper Cretaceous 'Rudist Formations'. Geol Pal ontol Mitt Innsburck 23:37–59

Sanders D (2001) Burrow-mediated carbonate dissolution in rudist biostromes (Aurisina, Italy): implications for taphonomy in tropical,

shallow subtidal carbonate environments. Palaeogeogr Palaeoclimatol Palaeoecol 168:39–74
Sanders D, Pons JM (1999) Rudist formations in mixed siliciclastic carbonate depositional environments, Upper Cretaceous, Austria: stratigraphy, sedimentology, and models of development. Palaeogeogr Palaeoclimatol Palaeoecol 148:249–284
Schlüter M, Steuber T, Parente M (2008) Chronostratigraphy of Campanian–Maastrichtian platform carbonates and rudist associations of Salento (Apulia, Italy). Cretac Res 29:100–114
Schmitt JG, Boyd DW (1981) Patterns of silicification in Permian pelecypods and brachiopods from Wyoming. J Sedimet Petrol 51:1297–1308
Scholle PA, Ulmer-Scholle DS (2003) A color guide to the petrology of carbonate rocks: grains, textures, porosity, diagenesis. AAPG Mem 77:461
Scoffin TP (1987) An introduction to carbonate sediments and rocks. Blackie, Glasgow, p 274
Selley RC (2000) Applied sedimentology. Academic Press, p 523
Shakeri AR (2013) Microfacies, depositional environment and diagenetic processes of the Mauddud Member, in a field in the Persian Gulf. J Geol Geosci 2(2):1–10
Sharland PR, Archer R, Casey DM, Davies RB, Hall SH, Heward AP, Horbury AD, Simmons MD (2001) Arabian plate sequence stratigraphy. GeoArabia, Special publication 2, Gulf PetroLink Bahrain, 371 p
Skelton PW (1974) Aragonite shell structures in the rudist Biradiolites and some palaeobiological inferences. Géol Méditerr 1:63–74
Skelton PW, El-Asa'ad GMA (1992) A new canaliculate rudist bivalve from the Aruma Formation of Central Saudi Arabia. Geol Romana 28:105–117
Steineke M, Bramkamp RA (1952) Stratigraphic introduction. In: Arkell WJ (ed) Jurassic ammonites from Jebel Tuwaiq, Central Arabia, vol 633. Phil. Trans. Royal Soc., London, pp 241–313
Steuber T (2002) A palaeontological database of rudist bivalves (Mollusca: Hippuritoidea, Gray 1848). http://www.paleotax.de/rudists/. Accessed 07.01.2002
Steuber T, Löser H (2000) Species richness and abundance patterns of Tethyan Cretaceous rudist bivalves (Mollusca: Hippuritacea) in the central-eastern Mediterranean and Middle East. Palaeogeogr Palaeoclimatol Palaeoecol 162:75–104
Steuber T, Özer S, Schlüter M, Sarı B (2009) Description of *Paracaprinula syriaca Piveteau* (Hippuritoidea, Plagioptychidae) and a revised age of ophiolite obduction on the African-Arabian Plate in southeastern Turkey. Cretac Res 30(1):41–48
Strohmenger CJ, Patterson PE, Al-Sahlan G, Mitchell JC, Feldman HR, Demko TM, Wellner RW, Lehmann PJ, Mccrimmon G, Broomhall RW, Al-Ajmi N (2006) Sequence stratigraphy and reservoir architecture of the Burgan and Mauddud formations (Lower Cretaceous), Kuwait. In: Harris PM, Weber LJ (eds) Giant hydrocarbon reservoirs of the world: from rocks to reservoir characterization and modeling. AAPG memoir 88, SEPM special publication, Tulsa, pp 213–245
Taghavi AA, Mork A, Emadi MA (2006) Sequence stratigraphically controlled diagenesis governs reservoir quality in the carbonate Dehluran Field, southwest Iran. Pet Geosci 12:115–126
Tibljaš D, Moro A, Ostrež Ž (2004) Mineral and chemical composition of rudist valves from Upper Cretaceous limestones of Southern Istria, Croatia. Geol Croat 57(1):73–79
Touir J, Soussi M (2003) The growth and migration of two Turonian rudistbearing carbonate platforms in Central Tunisia. Eustatic and tectonic controls. In: Gili E, Negra MH, Skelton PW (eds) Earth and environmental sciences: 28. North African Cretaceous Carbonate Platform Systems, Nato Science Series 4:53–81
Tucker M (1988) Techniques in sedimentology. Blackwell Scientific Publications, Oxford, p 394
Tucker ME, Wright VP (1990) Carbonate sedimentology. Blackwell Science, Hoboken 482 p
Vandeginste V, John CM, Manning C (2013) Interplay between depositional facies, diagenesis and early fractures in the Early Cretaceous Habshan Formation, Jebel Madar, Oman. Mar Pet Geol 43:489–503
Ziegler MA (2001) Late Permian to Holocene paleofacies evolution of the Arabian Plate and its hydrocarbon occurrences. GeoArabia 6(3):455–504